

# Impedance Control of Robots Using Voltage Control Strategy Revisited

Masoud Shahhosseini<sup>1\*</sup>

<sup>1</sup>Department of Electrical Engineering, Garmsar Branch, Islamic Azad University, Garmsar, Iran

\*Email of Corresponding Author: shahhosseini\_masoud@hotmail.com

*Received: August 6, 2018 ; Accepted: October 25, 2018*

## Abstract

In this note, we show that the impedance control strategy proposed in the paper is not feasible from practical implementation point of view. Next, a robust impedance controller is proposed for electrically driven robots using Fourier series (FS). The fact that robots' actuators have limited voltage is also considered in controller design procedure. In comparison with other impedance controllers using FS, the proposed controller results in fewer numbers of FS and consequently less computational load. These superiorities become more dominant when the manipulator degrees of freedom are increased. Simulation results on a Puma560 manipulator actuated by permanent magnet direct current electrical motors indicate the efficiency of proposed method.

## Keywords

Fourier series, Impedance control, Actuator saturation, Electrical driven robot, Voltage control strategy

## 1. Introduction

We have witnessed widespread industrial applications of robotic systems in which the interaction between the manipulator and environment should be managed automatically, such as assembly, polishing, grinding, mechanical part mating and also medical surgery. One of recent and high technological examples in this field is the exoskeleton robot [1, 2]. Simultaneous control of both motion and force is the main challenge in these applications [3, 4]. Many control laws have been developed to address this problem. However, it seems that impedance control [5, 6] and hybrid position/force control [7, 8] are the most important strategies [9-12]. In hybrid position/force control, one controller is responsible for position tracking in the free space and another controller is designed with the aim of force control along the directions in which position is constrained [13]. However, in impedance control, regulation of the dynamic performance of the system by careful selection of impedance parameters is considered. It is worthy to note that, almost all previous control strategies have ignored the actuator dynamics in their design procedure. In other words, their control laws calculate the desired torque that should be applied to the manipulator joints.

To cope with this problem, recently a voltage-based impedance controller has been developed considering actuator input signal constraint [1]. It has been assumed that, there is not any discrepancy between the nominal actuator parameters used in the impedance control law derivation and the true ones. In first view, it seems that the proposed voltage-based control strategy is very attractive, since it does not require any information from the manipulator dynamical model, the actuator mechanical subsystem, the inverse of the Jacobian matrix, and also its transpose. However,

some further considerations show that applying the voltage-based impedance control strategy for the actuated manipulator dynamics leads to a system with infinite-gain loop, which is not practical. Since impedance control requires the dynamical model of the manipulator, development of adaptive control algorithms is recommended to compensate for uncertainties. Many dynamical parameters of the manipulator such as mass and inertia of the links and the positions of the mass centers can be calculated using powerful software packages. Nevertheless, there may be some small errors and consequently, the calculated or measured quantities are just nominal values. As a result, if the structure of the system dynamics is known, then adaptive control is a suitable option to compensate for the parametric uncertainties such as the differences between the obtained nominal values and their unknown correct values [14].

Various adaptive impedance controllers have been developed in the last decades [15-23]. In [15], adaptive position control has been applied to robots that work in constraint environments. A model-free impedance control scheme has been developed in [16] using the framework of direct adaptive control. The information about the details of manipulators dynamic equations and also the parameters values are not required in this controller. To eliminate the need for acceleration signals, another adaptive impedance controller has been also designed in [17]. Neural networks have been also applied to adaptive impedance control. In [18], the matrices introducing the manipulator dynamics have been estimated in the controller using neural networks. Actuator dynamics have been excluded in this controller. Reinforcement learning approaches have been also applied to adaptive impedance control. A discrete-time Q-learning impedance controller has been developed in [19]. An impedance controller accompanied by passivity analysis has been presented in [20]. Based on nominal models of the manipulator, a hybrid impedance controller has been presented in [21]. For human-robot interactions, an impedance controller based on model reference strategy has been presented in [22]. With the aim of improving hybrid impedance control in complicated interaction tasks, a sliding mode controller has been designed in [23]. An important issue is that, most of these controllers require the regressor matrix. The reason is that these approaches utilize the property of linear parameterization. In addition, they cannot cope with unstructured uncertainty and external disturbance adequately, which is a significant disadvantage in almost all the addressed approaches. Recently, some adaptive controllers have been developed which are based on the FS or Legendre polynomials (LP) [24-32]. The main idea is representing the system uncertainties using orthogonal basis function such as FS, Bessel functions, LP, and etc. In this strategy, the regressor matrix is not required which consequently simplifies the controller design procedure. Moreover, acceleration signals are not needed in this strategy [33-34]. It is not recommended to use these signals in the control law, since they are usually contaminated by noise and will affect the system performance. However, requirement to weighting matrices with large dimensions makes its real-time computation consume too much time.

In this paper, a robust impedance controller is developed for electrically driven robot manipulators using FS. The MIMO structure of electrically driven robot is firstly modeled as a SISO system maintaining the coverage of interaction among joints and treating the coupling effect as uncertainty. In other word, we have  $n$  disturbed double integrator system. The lumped uncertainty is approximated by FS. Based on the stability analysis, some adaptation laws will then be obtained for the unknown coefficients of FS. The advantages of proposed controller over previous adaptive

controllers using FS are simplicity and less computational burden. Moreover, the required number of FS for uncertainty estimation is considerably reduced in the proposed method.

This paper is divided into 5 sections. After the introduction, section 2 discusses the main concerns regarding the voltage-based impedance control strategy implementation. The proposed impedance control design and stability proof are explained in section 3. Simulation results are illustrated in section 4 using a Puma560 robot manipulator actuated by geared permanent magnet dc motors and finally, conclusions are drawn in section 5.

## 2. Concerns Regarding Voltage-Based Impedance Control Strategy Implementation

Following the same notation as in the paper [1], the dynamic equation of an  $n$ -joint electrically driven robot interacted with the environment is described as [1]

$$\mathbf{D}(\mathbf{q})\ddot{\mathbf{q}} + \mathbf{C}(\mathbf{q}, \dot{\mathbf{q}})\dot{\mathbf{q}} + \mathbf{g}(\mathbf{q}) + \mathbf{J}^T(\mathbf{q})\mathbf{F}_{ext} = \boldsymbol{\tau}_l \quad (1)$$

$$\mathbf{J}_m \mathbf{r}^{-1} \ddot{\mathbf{q}} + \mathbf{B}_m \mathbf{r}^{-1} \dot{\mathbf{q}} + \mathbf{r} \boldsymbol{\tau}_l = \mathbf{K}_m \mathbf{I}_a \quad (2)$$

$$\mathbf{L} \dot{\mathbf{I}}_a + \mathbf{R} \mathbf{I}_a + \mathbf{K}_b \mathbf{r}^{-1} \dot{\mathbf{q}} = \mathbf{u}(t) \quad (3)$$

In which the parameters and also the signals are the same as those introduced in [1], with the same dimension. From practical point of view, the range of actuator input may limit by some upper and lower bound [35]. Suppose that the input limitation is described as

$$\mathbf{u}(t) = \text{sat}(\mathbf{v}(t)) \quad (4)$$

Where  $\mathbf{u}(t) = [u_1(t) \ u_2(t) \ \dots \ u_n(t)]^T$  is the actual actuator input,  $\mathbf{v}(t) = [v_1(t) \ v_2(t) \ \dots \ v_n(t)]^T$  is the controller output, and  $\text{sat}(\mathbf{v}(t)) = [\text{sat}(v_1(t)) \ \text{sat}(v_2(t)) \ \dots \ \text{sat}(v_n(t))]^T \in \mathfrak{R}^n$  represents the saturation function. When controller output falls out of linear range of the actuator operation, actuator saturation occurs. The non-implemented control signal by the device, denoted as  $\text{dzn}(\mathbf{v}(t), v_{\max})$ , is then given by [36]

$$\text{dzn}(\mathbf{v}(t), v_{\max}) = \mathbf{v}(t) - \text{sat}(\mathbf{v}(t)) \quad (5)$$

Where  $\text{dzn}(\mathbf{v}(t), v_{\max}) = [\text{dzn}(v_1(t), v_{1\max}) \ \dots \ \text{dzn}(v_n(t), v_{n\max})]^T \in \mathfrak{R}^n$  is the dead-zone function, and  $v_{\max} > 0$  is the maximum admissible voltage of the motor. Now, substituting (4) into (3) and using (5) we have

$$\mathbf{L} \dot{\mathbf{I}}_a + \mathbf{R} \mathbf{I}_a + \mathbf{K}_b \mathbf{r}^{-1} \dot{\mathbf{q}} = \mathbf{v}(t) - \text{dzn}(\mathbf{v}(t), v_{\max}) \quad (6)$$

Assume that actuators are in the linear operation area, i.e.,  $\mathbf{v}(t) = \mathbf{u}(t)$  [1]. It means that  $\text{dzn}(\mathbf{v}(t), v_{\max}) = 0$ . Now, our aim is to develop a control input  $\mathbf{v}(t)$ , such that the desired impedance relation can be achieved as follows

$$\mathbf{M}_R(\ddot{\mathbf{x}} - \ddot{\mathbf{x}}_d) + \mathbf{B}_R(\dot{\mathbf{x}} - \dot{\mathbf{x}}_d) + \mathbf{K}_R(\mathbf{x} - \mathbf{x}_d) = -\mathbf{F}_{ext} \quad (7)$$

Where  $\mathbf{M}_R \in \mathfrak{R}^n$  is the desired inertia,  $\mathbf{B}_R \in \mathfrak{R}^n$  is the desired damping, and  $\mathbf{K}_R \in \mathfrak{R}^n$  is the desired stiffness. It should be mentioned that these matrices are diagonal with positive constant elements. The actual task-space trajectories are denoted by  $\mathbf{x}$  and the desired task-space trajectories are denoted by  $\mathbf{x}_d$ . Also,  $\mathbf{F}_{ext}$  is the generalized force applied to the robotic arm by the environment and

$$\dot{\mathbf{x}} = \mathbf{J}(\mathbf{q})\dot{\mathbf{q}} \quad (8)$$

In which  $\mathbf{J}(\mathbf{q}) \in \mathfrak{R}^{n \times n}$  is the Jacobian matrix. With this in mind, we choose the same impedance control law as [1]

$$\mathbf{v}(t) = \mathbf{R}\mathbf{I}_a + \mathbf{L}\dot{\mathbf{I}}_a + \mathbf{K}_b \mathbf{r}^{-1} \mathbf{J}^{-1}(\mathbf{q}) \times (\dot{\mathbf{x}}_d - \mathbf{B}_R^{-1} \mathbf{F}_{ext} + \mathbf{B}_R^{-1} \mathbf{K}_R (\mathbf{x}_d - \mathbf{x})) \quad (9)$$

Where we assumed that  $\mathbf{x}_d$ , and  $\dot{\mathbf{x}}_d$  are all bounded, and  $\mathbf{M}_R = 0$  [1]. As it can be seen, feedbacks of  $\mathbf{x}$ ,  $\mathbf{q}$ ,  $\mathbf{I}_a$ , and  $\dot{\mathbf{I}}_a$  are required to implement the control law given by Equation (9). Moreover, it requires exact values of electrical resistance, electrical inductance, back EMF constant, gear-box ratio, and Jacobian matrix of the robotic system. Substituting the control law (9) into actuator electrical subsystem (6), and using (8), we have

$$\mathbf{B}_R(\dot{\mathbf{x}} - \dot{\mathbf{x}}_d) + \mathbf{K}_R(\mathbf{x} - \mathbf{x}_d) = -\mathbf{F}_{ext} \quad (10)$$

Which is a linear stable system. Consequently, all variables  $\mathbf{x} - \mathbf{x}_d$ , and  $\dot{\mathbf{x}} - \dot{\mathbf{x}}_d$  are bounded if  $\mathbf{F}_{ext}$  is bounded. Figure 1 illustrates a schematic diagram of the closed-loop system. For the sake of discussion, consider closed-loop controlled system proposed by [1] in the case where system is in the linear operation area as shown by Figure 2. Under this circumstance, we have

$$\mathbf{I}_a = (\mathbf{R} + \mathbf{L}s)^{-1} ((\mathbf{R} + \mathbf{L}s)\mathbf{I}_a + \mathbf{u}_{in}) \quad (11)$$

Or, equivalently

$$\mathbf{I}_a = \mathbf{I}_a + (\mathbf{R} + \mathbf{L}s)^{-1} \mathbf{u}_{in} \quad (12)$$

As can be seen, closed-loop control system includes an infinite-gain internal control loop that is not practical. This is the main concern in the aforementioned paper.

### 3. The Proposed Impedance Control Strategy

#### 3.1 Control law improvement

As mentioned in previous section, the voltage-based impedance controller [1] cannot be applied for the actuated robotic manipulator. Moreover, it does not consider the role of saturation function in controller design. To solve these problems, we extend the results obtained by [1]. Combining equations (1), (2) and (6), it follows that

$$\bar{\mathbf{D}}(\mathbf{q})\ddot{\mathbf{q}} + \bar{\mathbf{C}}(\mathbf{q}, \dot{\mathbf{q}})\dot{\mathbf{q}} + \bar{\mathbf{G}}(\mathbf{q}) + \mathbf{R}\mathbf{K}_m^{-1}\mathbf{r}\mathbf{J}^T(\mathbf{q})\mathbf{F}_{ext} = \mathbf{v}(t) - \mathbf{L}\dot{\mathbf{I}}_a - dzn(\mathbf{v}(t), v_{max}) \quad (13)$$

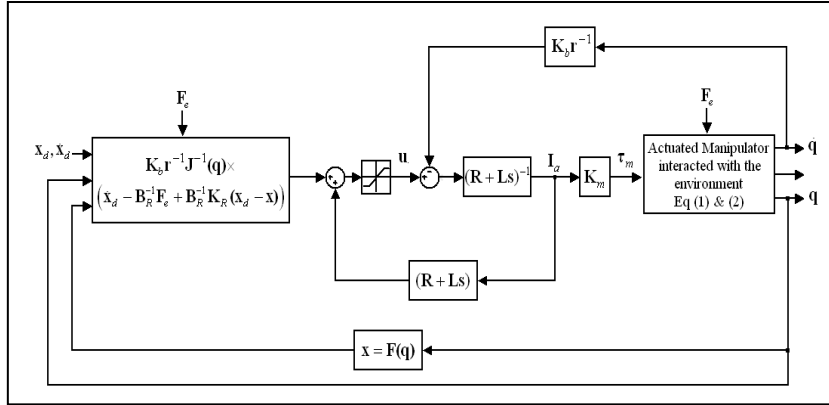


Figure1. Block diagram of the closed-loop controlled system using voltage control strategy

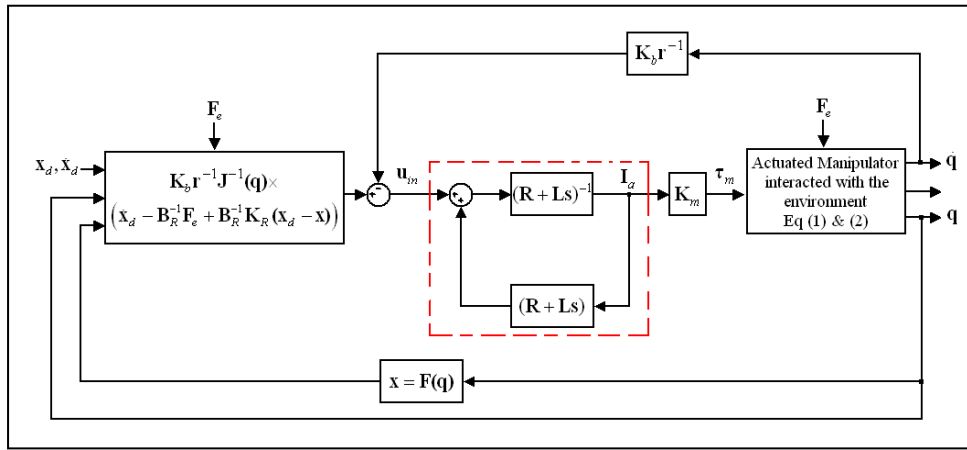


Figure2. Block diagram of the closed-loop controlled system using voltage control strategy (linear operation area)

Where the matrices  $\bar{\mathbf{D}}(\mathbf{q})$ ,  $\bar{\mathbf{C}}(\mathbf{q}, \dot{\mathbf{q}})$  and  $\bar{\mathbf{G}}(\mathbf{q})$  are completely described in [37]. It is desirable to describe the actuated manipulator dynamics in its operational space. Let the vector  $\mathbf{x} \in \mathfrak{R}^n$  be described as [8]

$$\mathbf{x} = \boldsymbol{\varphi}(\mathbf{q}) \quad (14)$$

In which  $\boldsymbol{\varphi}(\square) \in \mathfrak{R}^n \rightarrow \mathfrak{R}^n$  is generally a nonlinear mapping describing the transformation of the joint-space to the task-space. We can relate the task-space accelerations signals to those in the joint space by:

$$\ddot{\mathbf{x}} = \dot{\mathbf{J}}(\mathbf{q})\dot{\mathbf{q}} + \mathbf{J}(\mathbf{q})\ddot{\mathbf{q}} \quad (15)$$

Now, substituting (15) into (13), multiplying both sides by  $\mathbf{J}(\mathbf{q})^{-T}$ , and using (8), it follows that

$$\begin{aligned} \mathbf{M}(\mathbf{x})\ddot{\mathbf{x}} + \mathbf{H}(\mathbf{x}, \dot{\mathbf{x}})\dot{\mathbf{x}} + \mathbf{G}(\mathbf{x}) + \mathbf{J}(\mathbf{q})^{-T} \mathbf{R}\mathbf{K}_m^{-1}\mathbf{r}\mathbf{J}(\mathbf{q})^T \mathbf{F}_{ext} = \mathbf{v}(t) - \mathbf{J}(\mathbf{q})^{-T} \mathbf{L}\dot{\mathbf{I}}_a \\ - \mathbf{J}(\mathbf{q})^{-T} \text{dzn}(\mathbf{v}(t), v_{\max}) \end{aligned} \quad (16)$$

In which the matrices  $\mathbf{M}(\mathbf{x})$ ,  $\mathbf{H}(\mathbf{x}, \dot{\mathbf{x}})$ ,  $\mathbf{G}(\mathbf{x})$  and  $\mathbf{v}(t)$  are described in [38]. Now, we are ready to present the proposed robust impedance control strategy by introducing the following target impedance

$$\mathbf{M}_R(\ddot{\mathbf{x}}_t - \ddot{\mathbf{x}}_d) + \mathbf{B}_R(\dot{\mathbf{x}}_t - \dot{\mathbf{x}}_d) + \mathbf{K}_R(\mathbf{x}_t - \mathbf{x}_d) = -\mathbf{F}_{ext} \quad (17)$$

Where  $\mathbf{x}_t \in \mathfrak{R}^n$  denotes the task-space positions of the end-effectors in the reference model (17). The proposed controller is designed such that  $\mathbf{x} \rightarrow \mathbf{x}_t$  asymptotically, which yields convergence of the new target impedance (17) to (7) as desired. Toward this end, assume that equation (16) for the  $i$ th row can be described by

$$\ddot{x}_i = v_i(t) + \mathfrak{I}_i(t), \quad i = 1, 2, \dots, n \quad (18)$$

Where  $x_i$  is the  $i$ th element of vector  $\mathbf{x}$ , and

$$\begin{aligned} \mathfrak{I}_i(t) = (1 - m_{ii}(x))\ddot{x}_i - \sum_{j=1, j \neq i}^n m_{ij}(x)\ddot{x}_j - (\mathbf{H}(\mathbf{x}, \dot{\mathbf{x}})\dot{\mathbf{x}})_i - (\mathbf{G}(\mathbf{x}))_i \\ - (\mathbf{J}(\mathbf{q})^{-T} (\mathbf{R}\mathbf{K}_m^{-1}\mathbf{r}\mathbf{J}(\mathbf{q})^T \mathbf{F}_{ext} + \mathbf{L}\dot{\mathbf{I}}_a + \text{dzn}(\mathbf{v}(t), v_{\max})))_i, \quad i = 1, 2, \dots, n \end{aligned} \quad (19)$$

Before we go to the details of controller derivation, we present the two following assumptions.

Assumption 1. The singular positions are out of the operating range.

Assumption 2. Suppose that the nonlinear function  $\mathfrak{I}_i(t)$  is an unknown bounded function, and its variation bound is also assumed to be unavailable.

As a result of Assumption 2, traditional adaptive control scheme is not applicable. Based on these circumstances and assumptions, a proportional-derivative controller is designed in the form of

$$v_i(t) = -K_p x_i - K_d \dot{x}_i + K_p \wp_i, \quad i = 1, 2, \dots, n \quad (20)$$

In which the positive proportional and derivative scalar gains  $K_p$  and  $K_d$  are selected by the designer, and  $\wp_i$  is the new control input to be designed later. Substituting (19) into (18) leads to

$$\ddot{x}_i + K_d \dot{x}_i + K_p x_i = K_p \wp_i + \mathfrak{I}_i(t) \quad (21)$$

We now develop a procedure to calculate the control input  $\wp_i$ . To this end, we introduce a reference model as

$$\ddot{x}_i^d + K_d \dot{x}_i^d + K_p x_i^d = K_p \wp_i^d \quad (22)$$

Where  $\wp_i^d$  is the  $i$ th row of vector  $\mathbf{x}_t$ . Subtracting (22) from (21) results in

$$\ddot{\tilde{x}} + K_d \dot{\tilde{x}} + K_p \tilde{x} = K_p \mathfrak{N}_i + \mathfrak{S}_i(t) \quad (23)$$

Where  $\tilde{x}$  and  $\mathfrak{N}_i(t)$  are defined as

$$\tilde{x} = x_i - x_i^d, \quad \mathfrak{N}_i(t) = \wp_i(t) - \wp_i^d(t) \quad (24)$$

One can describe the system (23) in state space in the form of

$$\dot{\mathbf{h}} = \mathbf{A}\mathbf{h} + \mathbf{B}K_p \mathfrak{N}_i + \mathbf{B}\mathfrak{S}_i(t) \quad (25)$$

Where

$$\mathbf{A} = \begin{bmatrix} 0 & 1 \\ -K_p & -K_d \end{bmatrix}, \quad \mathbf{B} = \begin{bmatrix} 0 \\ 1 \end{bmatrix}, \quad \mathbf{h} = \begin{bmatrix} \tilde{x} \\ \dot{\tilde{x}} \end{bmatrix} \in \mathfrak{R}^2 \quad (26)$$

Now, our aim is finding a corrective control input  $\mathfrak{N}_i$  so that  $\mathbf{h}$  becomes bounded by a small positive constant or converges to zero. It has been assumed that we have not any knowledge about the actuator parameters and robot dynamic model. With this in mind, FS will be used to describe  $\mathfrak{S}_i(t)$  as linear combinations of sinusoidal functions as

$$\mathfrak{S}_i(t) = \mathbf{W}^T \mathbf{Z} + \varepsilon_{\mathfrak{S}_i} \quad (27)$$

Where  $\mathbf{W} \in \mathfrak{R}^r$  is weighting vector,  $\mathbf{Z} \in \mathfrak{R}^r$  is the vector of sinusoidal terms,  $\varepsilon_{\mathfrak{S}_i}$  is the truncation error of  $\mathfrak{S}_i(t)$  caused by considering a finite number of sinusoidal functions in the proposed FS and  $r$  represents the number of basis function used (sinusoidal functions). Making use the same set of basis functions, we proposed the corrective control input as

$$\mathfrak{N}_i(t) = -\frac{1}{K_p} \hat{\mathbf{W}}^T \mathbf{Z} \quad (28)$$

Where  $\hat{\mathbf{W}} \in \mathfrak{R}^r$  is an estimate of  $\mathbf{W}$ . When  $\mathfrak{N}_i(t)$  produced by (28), it should be translated into the main control input  $\wp_i(t)$  by

$$\wp_i(t) = \mathfrak{N}_i(t) + \wp_i^d(t) \quad (29)$$

Now, substituting (27) and (28) into (26), we obtain

$$\dot{\mathbf{h}} = \mathbf{A}\mathbf{h} + \mathbf{B}\tilde{\mathbf{W}}^T \mathbf{Z} + \mathbf{B}\varepsilon_{\mathfrak{S}_i} \quad (30)$$

In which  $\tilde{\mathbf{W}} = \mathbf{W} - \hat{\mathbf{W}}$  is error vector of the FS coefficients.

Theorem 1: Choose the parameters updating laws as

$$\dot{\hat{\mathbf{W}}} = \Gamma^{-1} (\mathbf{Z}\mathbf{B}^T \mathbf{P}\mathbf{h} - \sigma \hat{\mathbf{W}}) \quad (31)$$

Where  $\Gamma \in \mathfrak{R}^{Y \times Y}$  is positive definite constant matrix, and  $\sigma$  is positive constant. Then, the FAT-based tracking control laws (21), (28) and (29) for the  $i$ th subsystem (19), guarantee uniformly ultimately bounded stability of  $\mathbf{h}$ , and  $\tilde{\mathbf{W}}$ .

Proof: Consider a positive definite function as

$$V(\mathbf{h}, \tilde{\mathbf{W}}) = \mathbf{h}^T \mathbf{P} \mathbf{h} + \tilde{\mathbf{W}}^T \Gamma \tilde{\mathbf{W}} \quad (32)$$

Differentiating  $V(\mathbf{h}, \tilde{\mathbf{W}})$  along the trajectory of (28), and using (29), the inequality below can be obtained easily.

$$\dot{V}(\mathbf{h}, \tilde{\mathbf{W}}) = \mathbf{h}^T (\mathbf{A}^T \mathbf{P} + \mathbf{P} \mathbf{A}) \mathbf{h} + 2\mathbf{h}^T \mathbf{P} \mathbf{B} \varepsilon_{\mathfrak{S}_i} + 2\sigma \tilde{\mathbf{W}}^T \hat{\mathbf{W}} \quad (33)$$

It should be mentioned that  $\mathbf{A}$  is Hurwitz. As a result, symmetric positive definite matrices  $\mathbf{Q}$  and  $\mathbf{P}$  can be calculated based on the Lyapunov equation

$$\mathbf{A}^T \mathbf{P} + \mathbf{P} \mathbf{A} = -\mathbf{Q} \quad (34)$$

Thus, substituting (34) into (33) we have

$$\begin{aligned} \dot{V}(\mathbf{h}, \tilde{\mathbf{W}}) &= -\mathbf{h}^T \mathbf{Q} \mathbf{h} + 2\mathbf{h}^T \mathbf{P} \mathbf{B} \varepsilon_{\mathfrak{S}_i} + 2\sigma \tilde{\mathbf{W}}^T \hat{\mathbf{W}} \\ &\leq -\lambda_{\min}(\mathbf{Q}) \|\mathbf{h}\|^2 + 2\lambda_{\max}(\mathbf{P}) |\varepsilon_{\mathfrak{S}_i}| \|\mathbf{h}\| + 2\sigma (\tilde{\mathbf{W}}^T \mathbf{W} - \|\tilde{\mathbf{W}}\|^2) \end{aligned} \quad (35)$$

Result 1: Assume that number of sinusoidal functions is selected so that the truncation error is small and ignorable. Consequently, the  $\sigma$ -modification terms in (31) can be excluded. As a result, (35) can be simplified to

$$\dot{V}(\mathbf{h}, \tilde{\mathbf{W}}) \leq -\lambda_{\min}(\mathbf{Q}) \|\mathbf{h}\|^2 \quad (36)$$

And asymptotic convergence of  $\mathbf{h}$  will be obtained using the Barbalat's Lemma.

Result 2: If the truncation error  $\varepsilon_{\mathfrak{S}_i}$  in (35) cannot be ignored, the following procedure should be used. It is obvious that

$$\begin{aligned} -\lambda_{\min}(\mathbf{Q}) \|\mathbf{h}\|^2 + 2\lambda_{\max}(\mathbf{P}) |\varepsilon_{\mathfrak{S}_i}| \|\mathbf{h}\| &\leq -\frac{1}{2} \lambda_{\min}(\mathbf{Q}) \|\mathbf{h}\|^2 + \frac{2\lambda_{\max}^2(\mathbf{P})}{\lambda_{\min}(\mathbf{Q})} \varepsilon_{\mathfrak{S}_i}^2 \\ \tilde{\mathbf{W}}^T \mathbf{W} - \|\tilde{\mathbf{W}}\|^2 &\leq \frac{1}{2} (\|\mathbf{W}\|^2 - \|\tilde{\mathbf{W}}\|^2) \end{aligned} \quad (37)$$

Substituting these inequalities into (35) yields

$$\dot{V}(\mathbf{h}, \tilde{\mathbf{W}}) \leq -\frac{1}{2} \lambda_{\min}(\mathbf{Q}) \|\mathbf{h}\|^2 - \sigma \|\tilde{\mathbf{W}}\|^2 + \frac{2\lambda_{\max}^2(\mathbf{P})}{\lambda_{\min}(\mathbf{Q})} \varepsilon_{\mathfrak{S}_i}^2 + \sigma \|\mathbf{W}\|^2 \quad (38)$$

Note that

$$V(\mathbf{h}, \tilde{\mathbf{W}}) \leq \lambda_{\max}(\mathbf{P}) \|\mathbf{h}\|^2 + \lambda_{\max}(\Gamma) \|\tilde{\mathbf{W}}\|^2 \quad (39)$$

Then, (38) can be further derived as

$$\begin{aligned} \dot{V}(\mathbf{h}, \tilde{\mathbf{W}}) \leq & -\mu V + \left( \mu \lambda_{\max}(\mathbf{P}) - \frac{1}{2} \lambda_{\min}(\mathbf{Q}) \right) \|\mathbf{h}\|^2 \\ & + (\mu \lambda_{\max}(\mathbf{\Gamma}) - \sigma) \|\tilde{\mathbf{W}}\|^2 + \frac{2\lambda_{\max}^2(\mathbf{P})}{\lambda_{\min}(\mathbf{Q})} \varepsilon_{\mathfrak{S}_i}^2 + \sigma \|\mathbf{W}\|^2 \end{aligned} \quad (40)$$

By selecting  $\mu \leq \min \left\{ \frac{\lambda_{\min}(\mathbf{Q})}{2\lambda_{\max}(\mathbf{P})}, \frac{\sigma}{\lambda_{\max}(\mathbf{\Gamma})} \right\}$ , the second and third terms of (38) become negative, and thus

$$\dot{V}(\mathbf{h}, \tilde{\mathbf{W}}) \leq -\mu V + \frac{2\lambda_{\max}^2(\mathbf{P})}{\lambda_{\min}(\mathbf{Q})} \varepsilon_{\mathfrak{S}_i}^2 + \sigma \|\mathbf{W}\|^2 \quad (41)$$

The last equation is guaranteed to be negative whenever

$$V > \frac{2\lambda_{\max}^2(\mathbf{P})}{\mu\lambda_{\min}(\mathbf{Q})} \sup_{t_0 < \tau < t} \varepsilon_{\mathfrak{S}_i}^2(\tau) + \frac{\sigma}{\mu} \|\mathbf{W}\|^2 \quad (42)$$

Thus, it has been shown that the vectors  $\mathbf{h}$  and  $\tilde{\mathbf{W}}$  are uniformly ultimately bounded. ■

Because  $\mathbf{h}$  is bounded, boundedness of  $x_i$ , and  $\dot{x}_i$  can be obtained whereas  $x_i^d$  and  $\dot{x}_i^d$  are bounded. Moreover, applying this result to all subsystems gives boundedness of  $\mathbf{x}$  and  $\dot{\mathbf{x}}$ , respectively. Since the Jacobian matrix is bounded, boundedness of  $\dot{\mathbf{q}} = \mathbf{J}^{-1}(\mathbf{q})\dot{\mathbf{x}}$  can be obtained where as  $\dot{\mathbf{x}}$  is bounded. In addition to this,  $\mathbf{q} = \int_0^t \mathbf{J}^{-1}(\mathbf{q})\dot{\mathbf{x}} dt + \mathbf{q}(0)$  is also bounded for finite operational times. Therefore, the robotic system including manipulator and actuators will be stable, since boundedness all of system states have been guaranteed.

On the other hand, (41) also implies

$$V(\mathbf{h}, \tilde{\mathbf{W}}) \leq e^{-\mu(t-t_0)} V(t_0) + \frac{2\lambda_{\max}^2(\mathbf{P})}{\mu\lambda_{\min}(\mathbf{Q})} \sup_{t_0 < \tau < t} \varepsilon_{\mathfrak{S}_i}^2(\tau) + \frac{\sigma}{\mu} \|\mathbf{W}\|^2 \quad (43)$$

It is clear that the lower bound of  $V$  in (32) can be calculated in the form of

$$V(\mathbf{h}, \tilde{\mathbf{W}}) \geq \lambda_{\min}(\mathbf{P}) \|\mathbf{h}\|^2 + \lambda_{\min}(\mathbf{\Gamma}) \|\tilde{\mathbf{W}}\|^2 \quad (44)$$

This implies that  $\|\mathbf{h}\| \leq \sqrt{\frac{V(\mathbf{h}, \tilde{\mathbf{W}})}{\lambda_{\min}(\mathbf{P})}}$ . Together with (41), we have the bound for  $\mathbf{h}$  as

$$\|\mathbf{h}\| \leq \sqrt{\frac{V(t_0)}{\lambda_{\min}(\mathbf{P})}} e^{-\frac{\mu(t-t_0)}{2}} + \sqrt{\frac{2\lambda_{\max}^2(\mathbf{P})}{\mu\lambda_{\min}(\mathbf{P})\lambda_{\min}(\mathbf{Q})} \sup_{t_0 < \tau < t} |\varepsilon_{\mathfrak{S}_i}(\tau)|} + \sqrt{\frac{\sigma}{\mu\lambda_{\min}(\mathbf{P})}} \|\mathbf{W}\| \quad (45)$$

From (45), it is concluded that the magnitude of the  $\|\mathbf{h}\|$  is bounded. Its bound is given by some constants and an exponential function. In addition, from (45), it follows that by proper tuning of the controller parameters, the convergence rate of the tracking error can be improved. Hence,

$$\lim_{t \rightarrow \infty} \|\mathbf{h}\| \leq \sqrt{\frac{2\lambda_{\max}^2(\mathbf{P})}{\mu\lambda_{\min}(\mathbf{P})\lambda_{\min}(\mathbf{Q})}} \sup_{t_0 < \tau < t} |\varepsilon_{\mathfrak{S}_i}(\tau)| + \sqrt{\frac{\sigma}{\mu\lambda_{\min}(\mathbf{P})}} \|\mathbf{W}\| \quad (46)$$

Similarly, we can obtain the following upper bound for the vector  $\tilde{\mathbf{W}}$

$$\lim_{t \rightarrow \infty} \|\tilde{\mathbf{W}}\| \leq \sqrt{\frac{2\lambda_{\max}^2(\mathbf{P})}{\mu\lambda_{\min}(\mathbf{\Gamma})\lambda_{\min}(\mathbf{Q})}} \sup_{t_0 < \tau < t} |\varepsilon_{\mathfrak{S}_i}(\tau)| + \sqrt{\frac{\sigma}{\mu\lambda_{\min}(\mathbf{\Gamma})}} \|\mathbf{W}\| \quad (47)$$

Thus, the satisfactory performance of the controller in transient state is concluded. ■

#### 4. Simulation Results

In this section, simulations of a 6-DOF electrically driven robot are conducted to illustrate the performance of the proposed controller. Comparisons between the proposed controller and the voltage-based controller presented in [1] have also been done. To this end, a puma 560 robot manipulator with six revolute joints was selected. The corresponding dynamic model and kinematic parameters are found in [39-40]. The actuator dynamic model parameters are explained in [38]. According to [3], by selecting the roll, pitch, and yaw angles for describing the orientation of the end-effectors, the following rotation matrix is obtained:

$$\begin{aligned} [\mathbf{R}] &= \mathbf{R}_z(\alpha)\mathbf{R}_y(\beta)\mathbf{R}_x(\gamma) \\ &= \begin{bmatrix} \cos(\alpha)\cos(\beta) & \cos(\alpha)\sin(\beta)\sin(\gamma) - \sin(\alpha)\cos(\gamma) & \cos(\alpha)\sin(\beta)\cos(\gamma) + \sin(\alpha)\sin(\gamma) \\ \sin(\alpha)\cos(\beta) & \sin(\alpha)\sin(\beta)\sin(\gamma) + \cos(\alpha)\cos(\gamma) & \sin(\alpha)\sin(\beta)\cos(\gamma) - \cos(\alpha)\sin(\gamma) \\ -\sin(\beta) & \cos(\beta)\sin(\gamma) & \cos(\beta)\cos(\gamma) \end{bmatrix} \end{aligned} \quad (48)$$

Where the basic rotation matrices about the three coordinate axes are denoted by  $\mathbf{R}_x(\gamma)$ ,  $\mathbf{R}_y(\beta)$ , and  $\mathbf{R}_z(\alpha)$ . For each motor,  $u_{\max}$  is set to 60volts. Assume that a circle with the radius of 0.2m is defined as the desired trajectory for the manipulator end-effectors. The orientation was commanded to stay constant throughout the circular path. To put some constraints for the manipulator motion in the free space, suppose that a vertical wall is located at  $x_e = 0.55m$  along the y-axis. Assume that the stiffness of the wall is  $k_e = 5000 (N/m)$ . The environment dynamic was modeled as a regular spring, i.e.,  $f_{ext} = k_e(x - x_e)$  for  $x \geq x_e$ , where  $f_{ext}$  denotes for the force applied on the surface, and  $x$  is the coordinate of the end-point in the X direction. As a result, we have  $\mathbf{F}_{ext} = [f_{ext} \ 0 \ 0 \ 0 \ 0 \ 0]^T$ . The initial values of all joint positions are defined as  $q(0)=[2.3358 \ 1.5480 \ 0.1431 \ -1.6952 \ 0.7725 \ -0.6125]^T$ . The initial condition of the target impedance states is  $h_i(0)=[0.4 \ -0.2 \ 0.4 \ \pi/2 \ \pi/4 \ 0]^T$  that is the same as the initial value of the desired task-space trajectory. The target impedance matrices are selected to be  $\mathbf{B}_R = \text{diag}(100)_{6 \times 6}$ , and  $\mathbf{k}_R = \text{diag}(1500)_{6 \times 6}$ . Under these settings, the results of the voltage based impedance controller proposed by [1] have been illustrated in Fig. 3 to 4. Task-space tracking performance is represented in Figure 3. In addition, Figure 4 shows the applied voltage of

the actuators. As it can be seen, the control system presented in [1] cannot give suitable tracking trajectory, in spite of bounded control signal.

Due to comparison purpose, consider the impedance control strategy proposed in section 3. Suppose that the five first terms of FS are used, i.e.,  $\Upsilon = 5$ . Therefore,  $\hat{\mathbf{W}}_3 \in \mathfrak{R}^5$ . The initial values of the FS coefficients are set to zero. The gain matrices  $\Gamma$  (convergence rates of the FS coefficients) were chosen as diagonal matrices and were tuned manually  $\Gamma = 10^{-5} \times \mathbf{I}_5$  in which  $\mathbf{I}_{(\cdot)}$  is the identity matrix. First, it is assumed that the truncation error is ignorable. Therefore, the  $\sigma$ -modification parameters should be selected zero. Also, suppose that the target impedance matrices are defined as before, except that  $\mathbf{M}_R = \text{diag}(0.5)_{6 \times 6}$ . The controller parameters were chosen as  $K_p = 8000$ , and  $K_d = 80$  for all joints. It has been assumed that, matrices of  $\mathbf{M}(\mathbf{x})$ ,  $\mathbf{G}(\mathbf{x})$ ,  $\mathbf{H}(\mathbf{x}, \dot{\mathbf{x}})$ , and  $\mathbf{J}(\mathbf{q})$  are unknown.

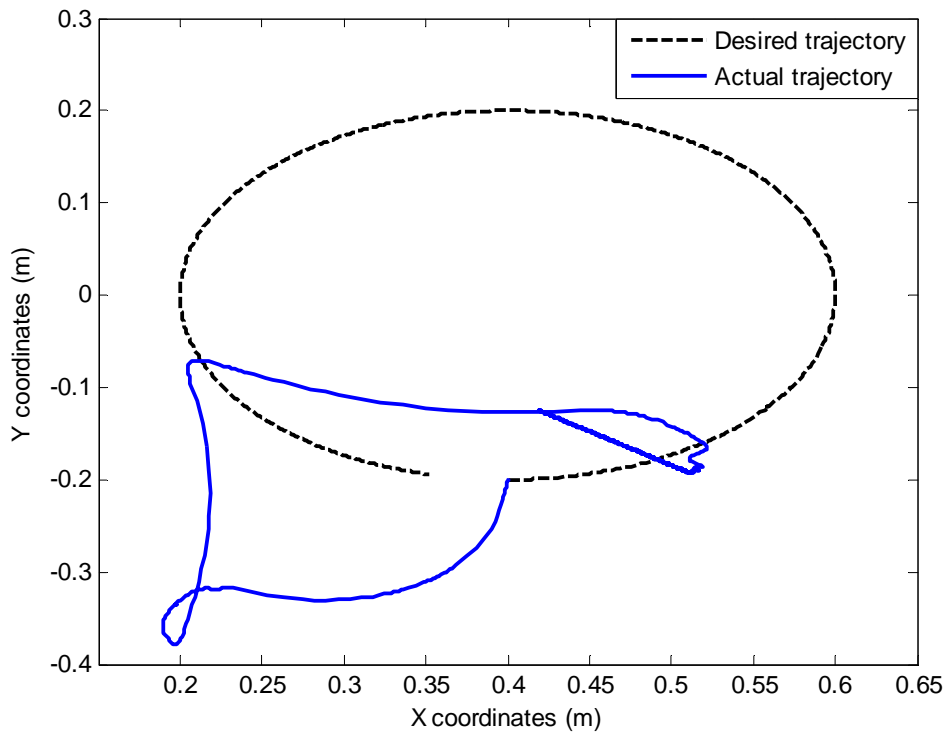


Figure3. Tracking performance of end point in the task space

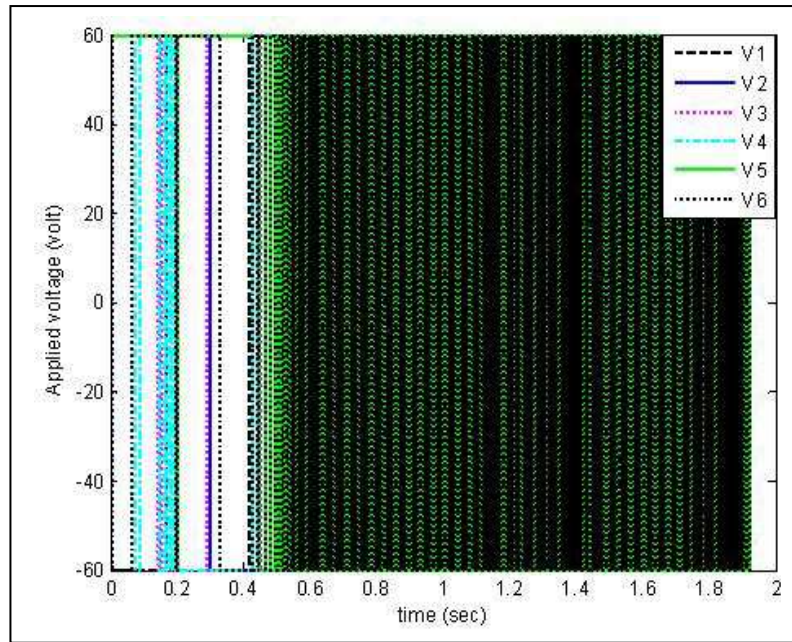


Figure4. Motor voltages

Under these settings, Figure 5 represents the desired trajectory and also the trajectory that the end-effectors have followed in the task-space. We are faced with different phases of operation. The reason is that the distance between the surface and the desired initial endpoint position is relatively large. The manipulator moves toward the wall without any constraint. Then, as it can be seen in Figure 6, the arm will interact with the wall around  $t=0.27\text{sec}$ . Because of collision,  $f_{ext}$  is generated. The end-effectors slide on the surface. Simultaneously, it exerts a force to the wall. The tracking error norms are plotted in Figure 7. According to this Figure, the steady state value of position error is in the range of  $2 \times 10^{-3}$  (m). The motor voltages computed by the proposed controller are satisfactory that can be seen in Figure 8. According to this Figure, the signals are smooth. Moreover, actuators are not saturated. Furthermore, computation of the high-dimensional complex regress or/weighting matrices is prevented in this algorithm that considerably simplifies the tuning procedure and also its practical implementation.

To show the role of corrective control input  $\kappa_i(t)$ , simulation is repeated without the presence of corrective term  $\kappa_i(t)$ . The tracking performance is degraded as shown in Figure 9. Tracking error norms for this case are plotted in Figure 10.

### 5 Conclusion

In this note, we showed that the voltage-based impedance control strategy proposed in the paper [1] cannot be applied for the actuated robotic manipulator. As an extension in the field of impedance controller design, a robust impedance controller using FS has also been proposed in this paper. Actuator saturation has been considered. Moreover, the controller has been designed so that the information of the system and environment are not required. Uncertainties have been estimated using FS. Satisfactory performance in the transient state has also been investigated. Simulation results on a Puma560 verify the efficiency of the proposed controller.

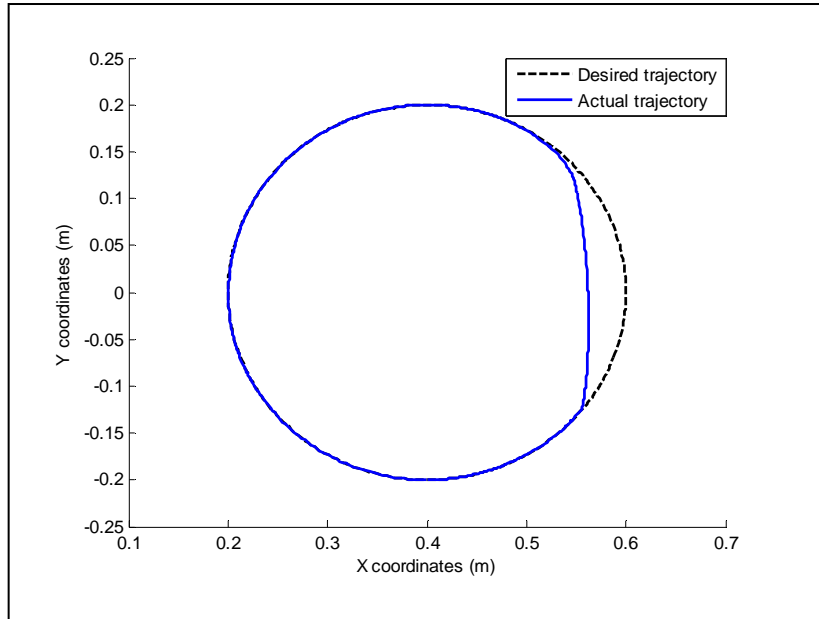


Figure5. Tracking performance of end point in the task space

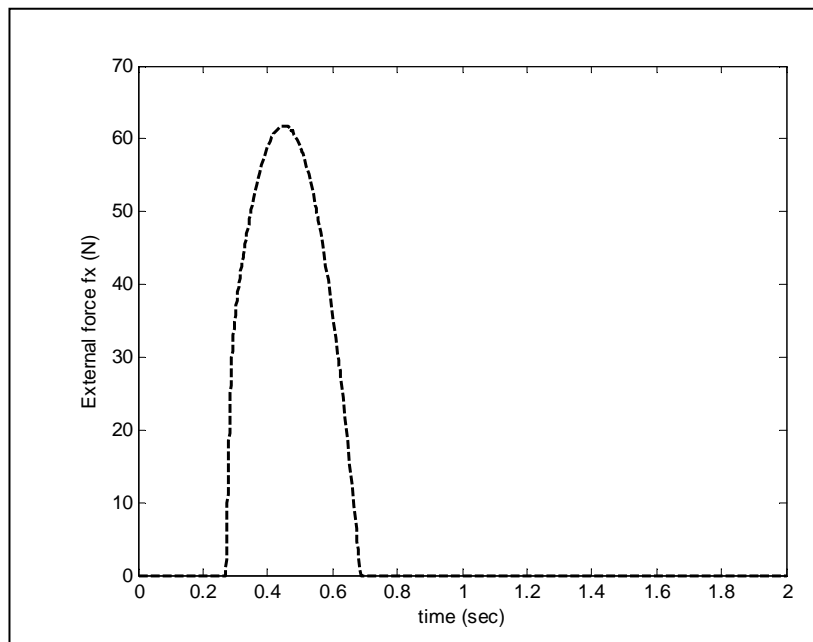


Figure6. External forces

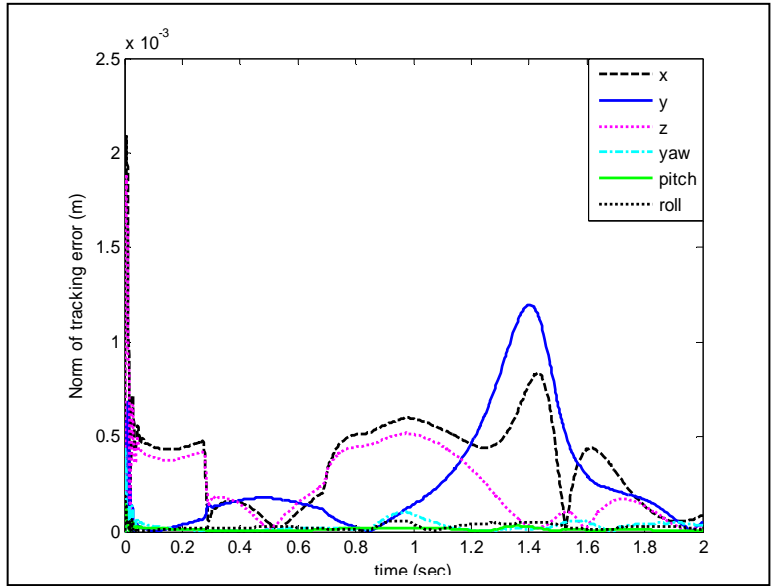


Figure7. Norm of tracking error

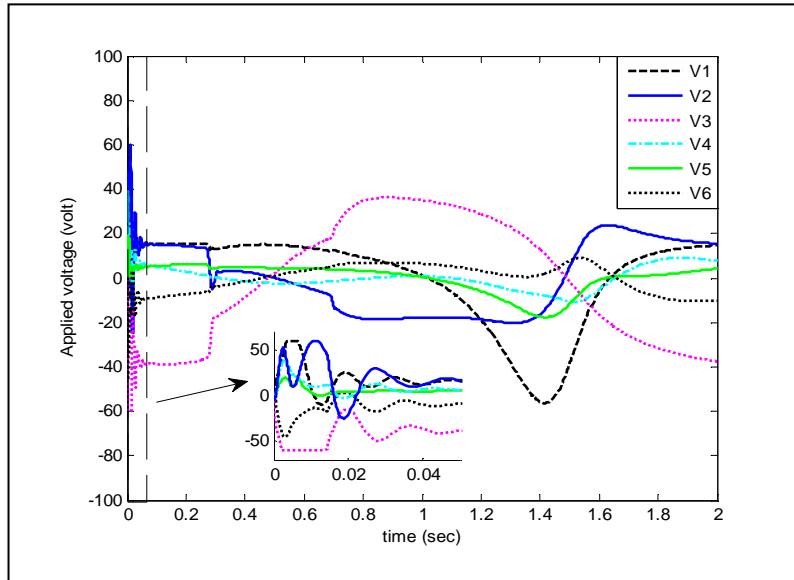


Figure8. Applied torques

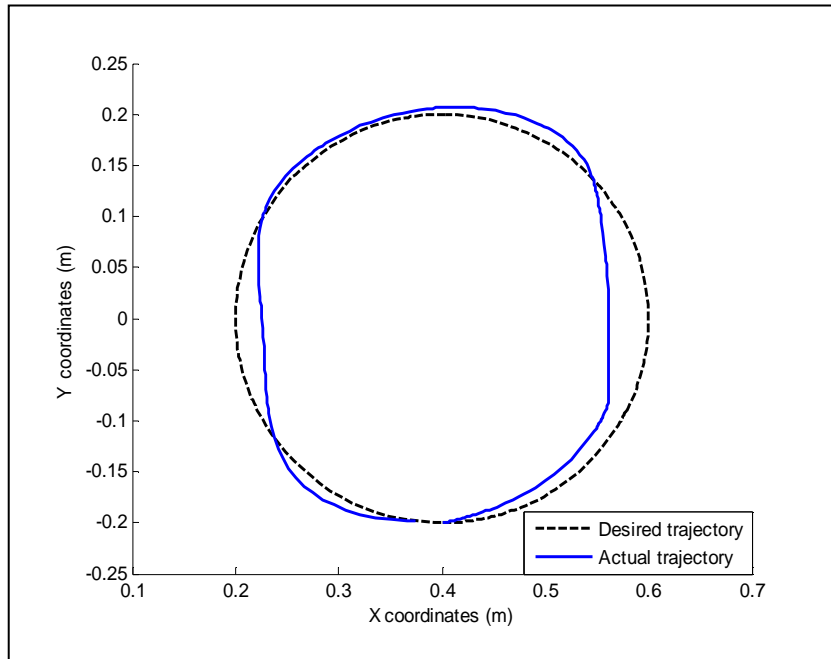


Figure9. Tracking performance of end point in the absence of auxiliary control input

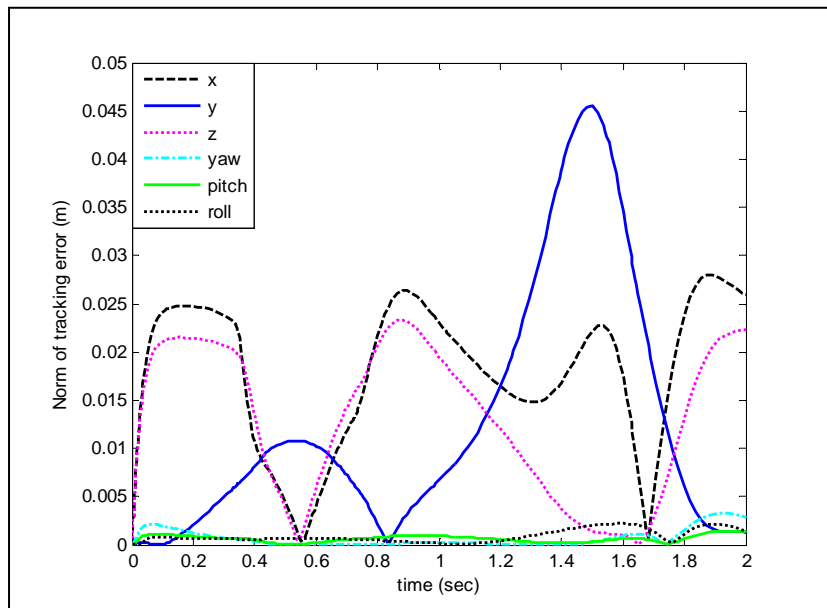


Figure10. Norm of tracking error in the absence of auxiliary control input

## 6. References

- [1] Fateh, M. M. and Babaghasabha, R. 2013. Impedance Control of Robots Using Voltage Control Strategy. *Nonlinear Dynamic*. 74(1-2): 277-286.
- [2] Mao, Y. and KAgrawal, S. 2012. Design of a Cable-Driven Arm Exoskeleton (CAREX) for Neural Rehabilitation. *IEEE Transactions on Robotics*. 28(4): 922-931.
- [3] Spong, M.W., Lewis, F. L. and Abdallah, C. T. 1993. *Robot Control: Dynamics, Motion Planning, and Analysis*. New York: IEEE Press.

- [4] Whitney, D. E. 1987. Historical Perspective and State of the Art in Robot Force Control. *International Journal of Robotics Research*. 6(1): 3-14.
- [5] Hogan, N. 1985. Impedance Control: an Approach to Manipulation: Part I-III. *ASME Journal of Dynamic Systems, Measurement and Control*. 107(1): 1-24.
- [6] Kazerooni, H. 1989. On the Robot Compliant Motion Control. *ASME Journal of Dynamic Systems, Measurement and Control*. 111(3): 416-425.
- [7] Raibert, M. and Craig, J . 1981. Hybrid Position/Force Control of Manipulators. *ASME Journal of Dynamic Systems, Measurement and Control*. 103(2): 126-133.
- [8] Khatib, O. 1987. A Unified Approach For motion and Force Control of Robot Manipulators: The Operational Space Formulation. *IEEE Journal of Robotics and Automation*. 3(1): 43-53.
- [9] Almeida, F., Lopes, A. and Abreu, P. 1999. Force-Impedance Control: A New Control Strategy of Robotic Manipulators. *Recent Advances in Mechatronics*. 1: 126-137.
- [10] Kazerooni, H., Houpt, P. and Sheridan, T. 1986. Robust Compliant Motion for Manipulators: Part II, Design method. *IEEE Journal on Robotics and Automation*. 2(2): 93-105.
- [11] Seraji, H. and Colbaugh, R. 1997. Force Tracking in Impedance Control. *The International Journal of Robotics Research*. 16(1): 97-117.
- [12] Boaventura, T., Buchli, J., Semini, C. and Caldwell, D. G. 2015. Model-Based Hydraulic Impedance Control For dynamic Robots. *IEEE Transactions on Robotics*. 31(6): 1324-1336.
- [13] Filaretov, V. F. and Zuev, A. V. 2008. Adaptive Force/Position Control of Robot Manipulators. *IEEE/ASME International Conference on Advanced Intelligent Mechatronics*. 96-101.
- [14] Spong, M. W., Hutchinson, S. and Vidyasagar, M. 2006. *Robot Modelling and Control*. Wiley, Hoboken.
- [15] Slotine, J. J. E. and Li, W. 1987. Adaptive Strategy in Constrained Manipulators. *Proc. IEEE International Conference on Robotics and Automation*. 595–601.
- [16] Colbaugh, R., Seraji, H. and Glass, K. 1991. Direct Adaptive Impedance Control of Manipulators. *Proc. IEEE Conference on Decision and Control*. 2410–2415.
- [17] Zhen, R. R. Y. and Goldenberg, A. A. 1995. An Adaptive Approach to Constrained Robot Motion Control. *Proc. IEEE International Conference on Robotics and Automation*. 1833–1838.
- [18] He, W., Dong, Y., and Sun, C. 2016. Adaptive Neural Impedance Control of a Robotic Manipulator with Input Saturation. *IEEE Transactions on Systems, Man, and Cybernetics: Systems*. 46(3): 334-344.
- [19] Yang, R., Yang, C., Chen, M., and Na, J. 2017. Adaptive Impedance Control of Robot Manipulators based on Q-learning and Disturbance Observer. *Systems Science & Control Engineering*. 5(1): 287-300.
- [20] Focchi, M., Medrano-Cerda, G. A., Boaventura, T., Frigerio, M., Semini, C., Buchli, J., and Caldwell, D. G. 2016. Robot Impedance Control and Passivity Analysis with Inner Torque and Velocity Feedback Loops. *Control Theory and Technology*. 14(2): 97-112.
- [21] Li, J., Liu, L., Wang, Y., and Liang, W. 2015. Adaptive Hybrid Impedance Control of Robot Manipulators with Robustness against Environment's Uncertainties. In *Mechatronics and Automation (ICMA), 2015 IEEE International Conference* . 1846-1851.

- [22] Sharifi, M., Behzadipour, S., and Vossoughi, G. 2014. Nonlinear Model Reference Adaptive Impedance Control for Human–Robot Interactions. *Control Engineering Practice*. 32: 9-27.
- [23] Wu, J., Fan, S., Shi, S., Li, Z., Jin, M., and Liu, H. 2017. Sliding Mode Hybrid Impedance Control of Manipulators for Complex Interaction Tasks. In *Advanced Intelligent Mechatronics (AIM), IEEE International Conference*. 1009-1014.
- [24] Huang, A.C. and Kuo, Y.S. 2001. Sliding Control of Nonlinear Systems Containing Time-Varying Uncertainties with Unknown Bounds. *International Journal of Control*. 74(3): 252–264.
- [25] Khorashadizadeh, S. and Fateh, M. M. 2015. Robust Task-Space Control of Robot Manipulators Using Legendre Polynomials for Uncertainty Estimation. *Nonlinear Dynamics*, 79(2): 1151-1161.
- [26] Huang, A.C., Wu, S.C. and Ting, W.F. 2006. A FAT-Based Adaptive Controller for Robot Manipulators without Regressor Matrix: Theory and Experiments. *Robotica*. 24(2): 205-210.
- [27] Chien, M.C. and Huang, A.C. 2012. Adaptive Impedance Controller Design for Flexible-Joint Electrically-Driven Robots without Computation of the Regressor Matrix. *Robotica*. 30(1): 133-144.
- [28] Khorashadizadeh, S., and Majidi, M. H. 2017. Chaos Synchronization Using the Fourier Series Expansion with Application to Secure Communications. *AEU-International Journal of Electronics and Communications*. 82(1): 37-44.
- [29] Chen, Y.F. and Huang, A.C. 2012. Controller Design for a Class of Underactuated Mechanical Systems. *IET Control Theory & Applications*. 6(1): 103-110.
- [30] Huang, A.C. and Chen, Y.C. 2004. Adaptive Multiple-Surface Sliding Control for Non-Autonomous Systems with Mismatched Uncertainties. *Automatica*. 40(11): 1939–1945.
- [31] Izadbakhsh, A. and Fateh, M. M. 2014. Real-time Robust Adaptive Control of Robots Subjected to Actuator Voltage Constraint. *Nonlinear Dynamics*. 78(3): 1999-2014.
- [32] Izadbakhsh, A. and Khorashadizadeh, S. 2017. Robust Impedance Control of Robot Manipulators Using Differential Equations as Universal Approximator. *International Journal of Control*. 1-17, DOI: <http://dx.doi.org/10.1080/00207179.2017.1336669>.
- [33] Chien, M. C. and Huang, A. C. 2004. Adaptive Impedance Control of Robot Manipulators based on Function Approximation Technique. *Robotica*. 22(4): 395-403.
- [34] Huang, A. C. and Chen, M. C. 2010. *Adaptive Control of Robot Manipulators: A Unified Regressor-Free Approach*. World Scientific.
- [35] Izadbakhsh, A., AkbarzadehKalat, A., Fateh, M. M. and Rafiei, S.M.R. 2011. A Robust Anti-Windup Control Design for Electrically Driven Robots-Theory and Experiment. *International Journal of Control, Automation and Systems*. 9(5): 1005-1012.
- [36] Izadbakhsh, A. 2016. Robust Control Design for Rigid-Link Flexible-Joint Electrically Driven Robot Subjected to Constraint: Theory and Experimental Verification. *Nonlinear Dynamic*. 85(2): 751-765.
- [37] Fateh, M. M. 2010. Proper uncertainty Bound Parameter to Robust Control of Electrical Manipulators Using Nominal Model. *Nonlinear Dynamics*. 61(4): 655-666.
- [38] Izadbakhsh, A. and Khorashadizadeh, S. 2017. Robust Task-Space Control of Robot Manipulators Using Differential Equations for Uncertainty Estimation. *Robotica*. 35(9): 1923-1938.

- [39] Armstrong, B., Khatib, O. and Bardick. J. 1986. The Explicit Dynamic Model and Inertial Parameters of the PUMA 560 arm. Proc. IEEE Robotics and Automation Conf., San Francisco, 510-518.
- [40] Corke, P. and Armstrong-Helouvry, B. 1994. A Search for Consensus Among Model Parameters Reported for the Puma560 Robot. IEEE Int. Conf. Robotics and Automation. 1608–1613.